A DIRECT DISCRETE-TIME OUTPUT FEEDBACK-BASED LS-RMRAC FOR GRID-TIED CURRENT CONTROL LOOP OF A STATIC 3-WIRE CONVERTER UNDER UNBALANCED GRID VOLTAGE CONDITIONS.[1]

Paulo Jefferson Dias de Oliveira Evald[2]

ABSTRACT

Nowadays, renewable energy generation is a worldwide tendency. These clean sources are generally tied to the grid by voltage-fed static converters. In this work, a direct discrete-time Output Feedback-based LS (Least Squares)-RMRAC (Robust Model Reference Adaptive Control) is proposed for grid-side current loop control of a static 3-wire converter connected to the grid through LCL filter. The proposed control method mitigates the LCL filter resonance, rejects grid disturbances without needing Resonant Controllers implementation, and deals properly with grid uncertainties and parametric variations, being suitable for grids with unbalanced voltage conditions. Simulation results of proposed controller are presented.

Keywords: Robust Adaptive Control. Grid-tied converter. LCL filter.

1 Introduction

Nowadays, fast society progress and growing industrial production have been demanding more and more energy. However, by use of conventional power generation, fossil fuels quickly will be shortened (FANG et al., 2019). Due to it and the global warming concerns, there is an increasing investment on renewable energy systems, such as: solar and wind farms, biomass power plant and ocean wave energy installations (ELSAYAD; MORADISIZKOOHI; MOHAMMED, 2018). However, even with all progress, there are still many remote locations in the world, which do not have access to electricity, or if have, it is a very restricted time connected in the grid (TIWARI; SINGH; GOEL, 2018). Moreover, a great portion of these places are rich in clean energy sources, which can be used to supply these remote areas sustainably through stand-alone power systems (NEHRIR et al., 2011).

Currently, there are over 400 GW of renewable energy generation worldwide, being around 300 GW by wind power and 100 GW by photovoltaic generation (ISLAM; GUO; ZHU,

---

[2] **Autor para correspondência:** Paulo Jefferson Dias de Oliveira Evald, paulo.evald@gmail.com

2013). It is highlighted that renewable energy-based stand-alone power systems of more than 10 MW in capacity, each power plant, already became a reality (ISLAM; GUO; ZHU, 2012). Therefore, renewable energy generators and distributed loads have emerged as an appealing solution for global development (RAHBAR; CHAI; ZHANG, 2016), from industrial requirements to remote village citizens needs. Thereby, power generation from renewable energy sources are becoming more and more pervasive in the energetic matrix (CRAMER et al., 2019).

Generally, power electronic converters are used to integrate primary source to the grid, and properly regulating the output power (KHWAN-ON; KONGKANJANA, 2017), with filters to reduce harmonics from converter switching. The two most popular filters used to interface grid and converter are L and LCL filters. Although L filter has a simpler structure and it is easier to design using active damping techniques, its major drawback is the reduced harmonics reduction in comparison to the LCL filter. Besides, LCL filter has reduced weight and size than L filter (TEODORESCU; LISERRE; RODRÍGUEZ, 2011). Moreover, LCL filter is cheaper; it allows lower switching frequency and has less reactive power consumption in the grid fundamental frequency (DANNEHL; FUCHS; THØGERSEN, 2010). In this work, a static 3-wire converter is simulated connected to the grid by an LCL filter.

The main drawback of the LCL filter is its resonance peak, which can cause controller performance degradation, and more, it can turn unstable the current loop control. In the literature, there are many approaches to mitigate LCL resonance peak by active damping. Among them, PI (Proportional Integral) controller (LINDGREN; SVENSSON, 1998; DANNEHL et al., 2010), virtual resistance-based PI controller (MOHAMMADI et al., 2019), PI plus repetitive controller (GAO et al., 2018), Optimal controller (MACCARI et al., 2015; TRAN; YOON; KIM, 2018), robust controller (OSÓRIO et al., 2019; GONZALEZ; BUSADA; SOLSONA, 2020), predictive controller (BOSCH; STAIGER; STEINHART, 2017; NAM et al., 2021), and others.

In general, fixed-gain controllers showed excellent performance only when the grid had no inductance changes (from strong to weak conditions), and the phases were equilibrated. However, grid inductance is always changing in practice, and their phases are not perfectly balanced, being necessary to use multi-loop fixed-gain control strategies to ensure energy quality. Alternatively, robust controllers designed with polytopic models can deal with grid uncertainties without multi-loop control laws, as proposed on (MACCARI et al., 2013; OSÓRIO et al., 2019; JUNIOR et al., 2020; BELOV, 2022). These controllers presented high performance in the current control, even when the grid was unbalanced. However, the design of this kind of controller requires a lot of experience with LMI (Linear Matrix Inequalities), which is a non-trivial technique. Furthermore, the performance of a robust controller is highly dependent on the plant model. Thereby, although these methods have presented good performance on grid-

injected current control at non-nominal conditions, the main drawback for all is the same: their gains are fixed values. This characteristic restricts their operational point and do not guarantee performance for parametric variations outside designed operational range (FLORA; GRÜN-DLING, 2008). Therefore, in this work is presented an adaptive controller solution, which can properly deal with variable operational points and more, it can deal with exogenous disturbance from the grid without needing Proportional Resonant controllers, avoiding multi-loop controllers. The proposed strategy to control grid-side currents of a static 3-wire converter is a direct discrete-time Output Feedback-based LS (Least Squares)-RMRAC (Robust Model Reference Adaptive control). Simulation results including converter switching, implementation delay, voltage grid synchronization and pulse width modulation through Space Vector method are presented to validate the controller performance. Besides, voltage grid synchronization is performed with a Kalman filter, eliminating the need for using a conventional phase-lock loop. Moreover, parametric variations in grid impedance and unbalanced grid voltage conditions are also considered.

This work is organized as follows: Section II gives the mathematical model of a grid-tied static 3-wire converter with LCL filter. Next, in the Sections III and IV are presented controller design and simulation results, respectively. Lastly, in Section V, the final considerations of this work are presented.

2   Grid-tied Static 3-wire Converter with LCL filter

A renewable energy power system consists of four main subsystems: a clean power source generator (generally sun, wind, ocean waves, or biomass), a power converter, a capacitor bank, and AC filter. In the simulations, the clean power source was approximated to a continuous-voltage source, V_{CC}, which can represent the sun in a photovoltaic system. In addition, the electrical grid was assumed to be predominantly inductive, modeled by a sinusoidal source V_d, as presented Figure 1. The grid impedance is represented by inductance L_{g2} and parasitic resistance R_{g2}, in series with the grid, V_d. Besides, the LCL circuit was represented by the Thevenin equivalent in relation to the PCC (Point of Common Coupling) (TAMBARA et al., 2017). The LCL parameters, shown in Figure 1, are: i_c, v_c and i_g, which are converter-side currents, capacitor voltage and grid-side currents, respectively. It is noteworthy to emphasize that total grid-side inductance and total grid-side resistance are given by $L_g = L_{g1} + L_{g2}$ and $R_g = R_{g1} + R_{g2}$, respectively. Also, R_c and L_c are the converter resistance and inductance, respectively.

It is known that resulting model in three-phase coordinates is coupled and design an active damping method for it is a hard and complex task (EVALD; TAMBARA; GRÜNDLING,
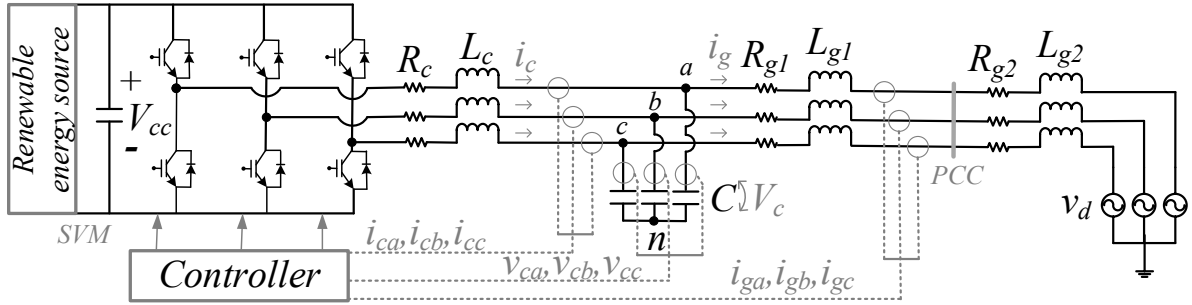
Figure 1 – Grid-tied static 3-wire converter with LCL filter in three-phase coordinates
Fonte: The author.

2020a). Therefore, Clarke Transform (DUESTERHOEFT; SCHULZ; CLARKE, 1951) was applied on three-phase coordinates model, obtaining two identical decoupled single-phase linear time-invariant (LIT) models (TAMBARA et al., 2017), which are equivalent and preserve current and voltage amplitude. Note that, if grid phases are equilibrated, then there is no path for current conduction on the 0 axis; therefore, it can be disregarded. However, here, the grid is considered unbalanced; thence, there will be current flowing in the 0 axis. In this situation, a fixed-gain controller does not guarantee good performance and stability; once, for a 3-wire converter, it has no access to control 0 axis. However, it is shown that even under these unfavorable conditions, and more, considering parametric variation in one of the grid phases, the proposed controller is robust enough to maintain the closed-loop system stable, with small tracking error, which is feasible for experimental implementation. The transfer function, $G(s)$, of identical decoupled models in $\alpha\beta$ coordinates, taking into account that the converter is disconnected from the grid $v_d = 0$, because the grid is the exogenous disturbance for the current controller, is given by

$$G(s) = \frac{i_g(s)}{u(s)} = \frac{\dfrac{1}{L_g L_c C}}{s^3 + \dfrac{(R_g L_c + R_c L_g)}{L_g L_c}s^2 + \dfrac{(L_c + L_g + R_g R_c C)}{L_g L_c C}s + \dfrac{R_g + R_c}{L_g L_c C}} \tag{1}$$

where $u(s)$ is the voltage synthesized by the converter through Space Vector Modulation (SVM) technique. Moreover, implementation delay was considered in the simulation. To do it, the control action is implemented with a delay of 1 time step, that is, $u(k) = u(k-1)$.

3 Direct Discrete-time Output Feedback-based LS-RMRAC

First of all, assuming that a continuous-time plant was properly discretised, a discrete-time SISO (Single Input Single Output) plant $G(z)$ can be described as

$$G(z) = G_0(z)[1 + \mu\Delta_m(z)] + \mu\Delta_a(z), \tag{2}$$

where $\Delta_m(z)$ and $\Delta_a(z)$ are a multiplicative and an additive dynamics, respectively (EVALD; TAMBARA; GRÜNDLING, 2020b). Also, $G_0(z)$ is the modeled part of the plant, which is described by

$$G_0(z) = k_p \frac{Z_p(z)}{R_p(z)}, \qquad (3)$$

where k_p is the high frequency gain of $G_0(z)$, $Z_p(z)$ and $R_p(z)$ are monic polynomials of degrees m and n, respectively.

The additive and multiplicative dynamics jointly with modeled part of the plant must satisfy the following assumptions (IOANNOU; SUN, 2012),
A1) $Z_p(z)$ is a Schur polynomial and the high frequency gain signal is known;
A2) $\Delta_a(z)$ is a strictly proper Schur transfer function, and $\Delta_m(z)$ is a Schur transfer function;
A3) The upper bound on stability margin of $\Delta_a(z)$ and $\Delta_m(z)$ is internal to the unit Z circle.

In reference model-based adaptive controllers, it does not track the reference signal directly; that is, the plant output is forced to track the reference model output, as close as possible. The reference model, $W_m(z)$, is designed with the same relative degree of $G_0(z)$ as follows

$$y_m = W_m(z)r = k_m \frac{Z_m(z)}{R_m(z)}r, \qquad (4)$$

where k_m is the high frequency gain of $W_m(z)$, $Z_m(z)$ and $R_m(z)$ are monic Schur polynomials with degrees m^* and n^*, respectively. In addition, $y_m(k)$ and $r(k)$ are the reference model output and a bounded reference signal, respectively. There is only one assumption for reference model, which is:
A4) $R_m(z)$ is an arbitrary Schur monic polynomial of relative degree $n^* = n - m > 0$.

The control action $u_(k)$ is extracted from $\boldsymbol{\theta}^T(k)\boldsymbol{\omega}(k) + r(k) = 0$, where $\boldsymbol{\theta}(k)$ is the adaptive gains vector and $\boldsymbol{\omega}(k)$ is a vector formed by internal filters, plant output, reference signal and disturbance rejection terms. The $\boldsymbol{\omega}(k)$ consists in the following structure

$$\boldsymbol{\omega}^T(k) = [\ \boldsymbol{\omega}_1^T(k)\ \boldsymbol{\omega}_2^T(k)\ y(k)\ u(k)\ V_s(k)\ V_c(k)\ ], \qquad (5)$$

where $\boldsymbol{\omega}_1(k)$ and $\boldsymbol{\omega}_2(k)$ are reconstructive filters, $y(k)$ is plant output, $V_s(k)$ and $V_c(k)$ are phase and quadrature components of exogenous disturbance, respectively. The internal filters are

$$\begin{aligned} \boldsymbol{\omega}_1(k+1) &= (\boldsymbol{I} + \boldsymbol{F}T_s)\boldsymbol{\omega}_1(k) + \boldsymbol{q}T_s u(k), \\ \boldsymbol{\omega}_2(k+1) &= (\boldsymbol{I} + \boldsymbol{F}T_s)\boldsymbol{\omega}_2(k) + \boldsymbol{q}T_s y(k), \end{aligned} \qquad (6)$$

where $\boldsymbol{I}$ is an identity matrix of dimensions $n \times n$ and $(\boldsymbol{F}, \boldsymbol{q})$ is a controllable pair with a stable matrix $\boldsymbol{F}$ and a vector of controllable parameters $\boldsymbol{q}$, with dimensions $n - 1 \times n - 1$ and $n - 1$, respectively (IOANNOU; TSAKALIS, 1986). In addition, T_s is the sampling time.

A Least Square algorithm (IOANNOU; SUN, 2012) was utilized for gains adaptation of controller:

$$\boldsymbol{\theta}(k+1) = \boldsymbol{\theta}(k) - T_s\sigma(k)\boldsymbol{P}(k)\boldsymbol{\theta}(k) - T_s\kappa\boldsymbol{P}(k)\frac{\boldsymbol{\zeta}(k)\varepsilon(k)}{m^2(k)}, \tag{7}$$

where $\boldsymbol{P}(k)$ is the covariance matrix, κ is a positive parameter that accelerates parametric convergence pondering the augmented error ε, which is

$$\varepsilon(k) = y(k) + \boldsymbol{\theta}^T(k)\boldsymbol{\zeta}(k), \tag{8}$$

where $\boldsymbol{\zeta}(k)$ is the $\boldsymbol{\omega}(k)$ filtered by reference model,

$$\boldsymbol{\zeta} = W_m(z)\boldsymbol{\omega}. \tag{9}$$

The parametric convergence is defined by covariance matrix $\boldsymbol{P}(k)$, which is computed as

$$\boldsymbol{P}(k+1) = \boldsymbol{P}(k) - T_s\boldsymbol{P}(k)\boldsymbol{\zeta}(k)\boldsymbol{\zeta}^T(k)\boldsymbol{P}(k) + T_s\beta\iota, \tag{10}$$

where ι is a matrix of ones and the term $T_s\beta\iota$ is a modification on LS algorithm to prevent $\boldsymbol{P}$ to stagnate in zero. If it occurs, parameters are no longer adapted and the tracking error can be increased to an unacceptable level.

Furthermore, σ-modification was used to improve robustness into adaptive controller. It is a projection method that limits parameters increasing by their norm,

$$\sigma(k) = \begin{cases} 0 & \text{if} \quad \|\boldsymbol{\theta}(k)\| < M_0 \\ \sigma_0\left(\dfrac{\|\boldsymbol{\theta}(k)\|}{M_0} - 1\right) & \text{if} \quad M_0 \le \|\boldsymbol{\theta}(k)\| < 2M_0, \\ \sigma_0 & \text{if} \quad \|\boldsymbol{\theta}(k)\| \ge 2M_0 \end{cases} \tag{11}$$

where $M_0 > \|\boldsymbol{\theta}^*\|$ is the upper limit of $\boldsymbol{\theta}(k)$ norm, securely oversized due to lack of knowledge of $\|\boldsymbol{\theta}(k)^*\|$ and σ_0 is the maximum value of the modification function (EVALD; TAMBARA; GRÜNDLING, 2020b).

Moreover, a majorant signal $m^2(k)$, similar to a normalizer, was also implemented to ensure robustness to the adaptive controller. Here, it was designed as shown in (EVALD; TAMBARA; GRÜNDLING, 2020a),

$$m^2(k) = 1 + \boldsymbol{\zeta}^T(k)\boldsymbol{\zeta}(k). \tag{12}$$

The block diagram of presented control method is shown in Figure 2, where $e_1(k)$ is the tracking error, calculated as the difference between plant and reference model outputs, $e_1(k) = y(k) - y_m(k)$.
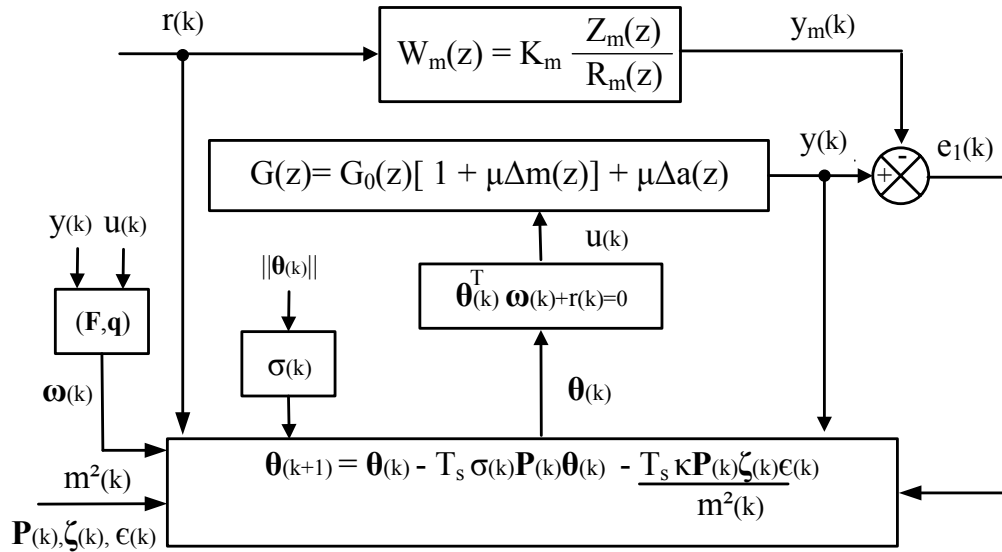
Figure 2 – Block diagram of proposed controller
Fonte: The author.

4   Simulation Results

Simulations of the closed-loop system were carried out in the Octave 6.1, and they include converter switching dynamics, governed by SVM (PINHEIRO et al., 2005), to synthesis the control action. Also, the controller was synchronized with the grid voltage by a Kalman Filter algorithm (CARDOSO et al., 2008). Furthermore, grid voltages, which were estimated with Kalman filter, are also used to identify phase and quadrature of grid disturbance, with the aim of rejecting it, and to generate a reference signal. It is highlighted that, for some cycles, while initial synchronization occurred, the converter was maintained inhibited.

The grid frequency, line voltage range and DC bus voltage were set to 60 Hz, 110 V and 250 V, respectively. Besides, the converter's switching frequency and the controller's sampling frequency were both set to 5 kHz. The parameters of grid and LCL filter are shown in the Table 1, which is identical to the experimental setup of (EVALD; TAMBARA; GRÜNDLING, 2020b).

The reference model was chosen to have unit gain in steady state regime and presents fast dynamics. It is identical for both coordinates, given as follows,

$$W_m(z) = \frac{0.343}{(z-0.3)^3}. \tag{13}$$

Due to the adaptive nature of the controller, the controller parameters can be chosen empirically over a large range, which will convergence to a set of parameters that minimizes the tracking error in steady state. The LS parameters were determined through a set of simulations, aiming for fast tracking and low overshoot. The resulting values are: $\boldsymbol{P}(0) = 100\boldsymbol{I}$,

Table 1 – Grid and LCL filter parameters

Symbol	Parameter	Value	Symbol	Parameter	Value
L_c	Converter-side inductance	1 mH	L_{g2}	Grid inductance (phase a)	0.45 mH
R_c	Converter-side resistance	50 mΩ	L_{g2}	Grid inductance (phase b)	0.50 mH
C	Capacitance of LCL filter	62 μF	L_{g2}	Grid inductance (phase c)	0.55 mH
L_{g1}	Grid-side inductance	0.3 mH	R_{g2}	Grid resistance	50 mΩ
R_{g1}	Grid-side resistance	50 mΩ			

Fonte: The author.

$\beta = 50$ and $\kappa = 15$. These parameters determine the convergence rate: as higher they are, the faster will be the parametric convergence. However, if they are chosen with excessively high values, the algorithm can impose an oscillatory behavior to $\boldsymbol{\theta}$ gains, and, consequently, they can not converge. In the future steps of this study, the design constraints will be determined through Lyapunov' stability criterion. Besides, the parameters of σ-modification were chosen as $\sigma_0 = 0.1$ and $M_0 = 10$, which can be oversized due to unknown norm of $\boldsymbol{\theta}$ (EVALD; TAMBARA; GRÜNDLING, 2020b). Moreover, the initial value of majorant signal was chosen as one, $m^2(0) = 1$, to avoid division by zero on $\boldsymbol{\theta}(1)$ computation, once it will be continuously recalculated based on $\boldsymbol{\zeta}$ dynamics. Finally, the pair $(\boldsymbol{F}, \boldsymbol{q})$ was set to $\boldsymbol{F} = 1000\boldsymbol{I}$ and $\boldsymbol{q} = [1000\ 0]$ to impose a soft dynamics on internal filters $\boldsymbol{\omega}$.

Moreover, all parameters of $\boldsymbol{\zeta}$ and $\boldsymbol{\omega}$ were initialized as zero. In addition, to avoid excessive overshoot in the initial transient regime, a previous simulation was performed, considering the designed controller parameters, using a reference sinusoidal signal with an amplitude of 10 A and a frequency of 60 Hz, without grid impedance variation. The final gain values achieved in this simulation were taken to initialize $\boldsymbol{\theta}(0)$ vector of presented simulation. These values are

$$
\boldsymbol{\theta}_\alpha(0) = \begin{bmatrix} -1.8569897 \\ 0 \\ -0.71954155 \\ 0 \\ -1.1173636 \\ -1.9491602 \\ 3.8845067 \\ -0.36709696 \end{bmatrix}, \quad \boldsymbol{\theta}_\beta(0) = \begin{bmatrix} -0.71336466 \\ 0 \\ -0.35032609 \\ 0 \\ -0.88017768 \\ -1.2983845 \\ 1.8041753 \\ -0.3386625 \end{bmatrix}.
$$

The initial reference current has an amplitude equal to 15 A. At 0.1 s, this amplitude is increased to 25 A. In addition, at 0.15 s, a parametric variation on grid impedance is imposed, by adding 0.4 mH with 50 mΩ only on phase a, unbalancing more the grid. Figure 3 shows

grid-side currents in three-phase coordinates, followed by currents tracking in $\alpha\beta$ coordinates on Figure 4.
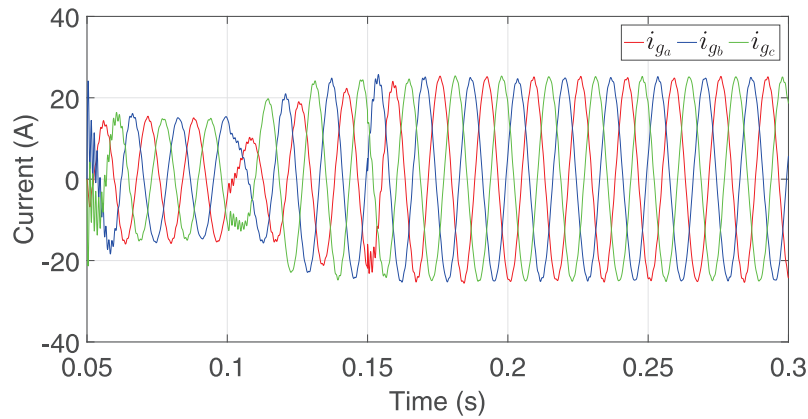
Figure 3 – Grid-side currents in *abc* coordinates
Fonte: The author.
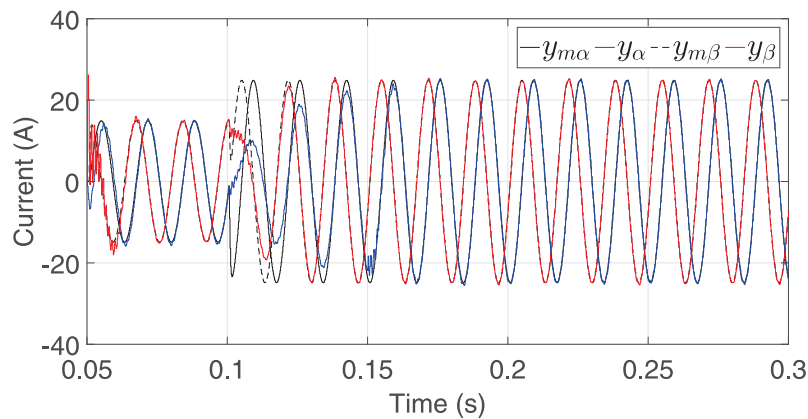
Figure 4 – Grid-side currents in $\alpha\beta$ coordinates
Fonte: The author.

As can be observed on Figure 3, the grid-injected currents presented a well-controlled behavior. The reference tracking occurred very quickly, as can be better seen on $\alpha\beta$ coordinates, shown on Figure 4, with short transient response, which was around two grid cycles. It can be noted that currents were very close to the reference model outputs, even when parametric variation was imposed on the grid impedance. Moreover, the controller dealt properly with exogenous disturbances from the electrical grid. The tracking errors are shown in Figure 5. Note that tracking errors are greater on initial transient regime, due to grid uncertainties, which forced the gains to readapt, as well as at reference change instant, because it imposed a great active power output increase. The gains in adaptation $\boldsymbol{\theta}(k)$ are shown in Figures 6 and 7, for α and β coordinates, respectively.
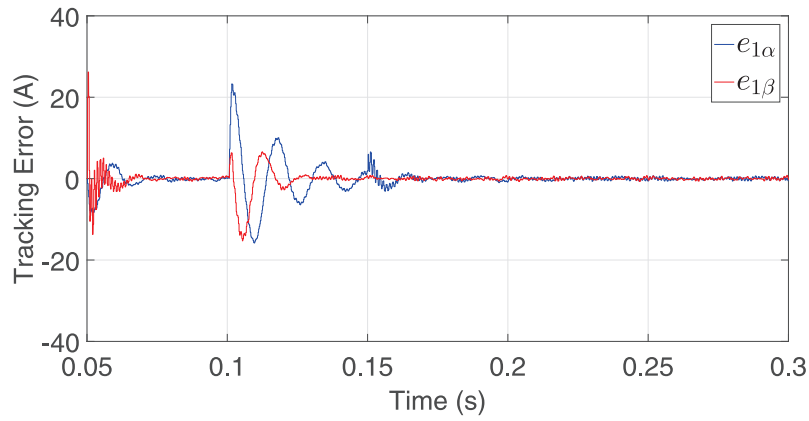
Figure 5 – Tracking errors in αβ coordinates
Fonte: The author.
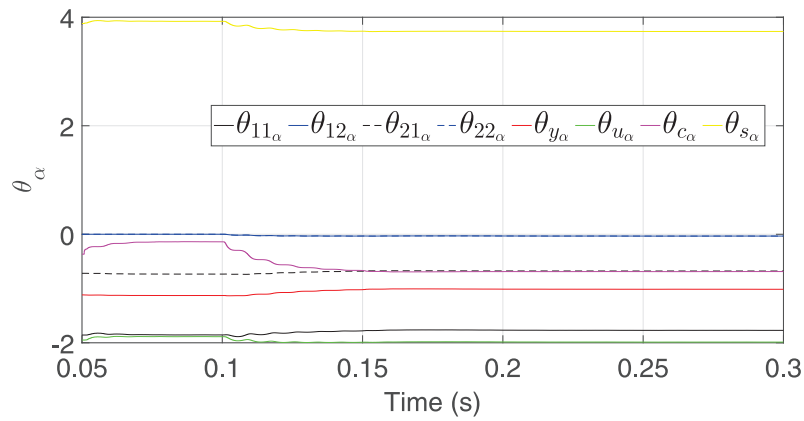
Figure 6 – Gains in α
Fonte: The author.
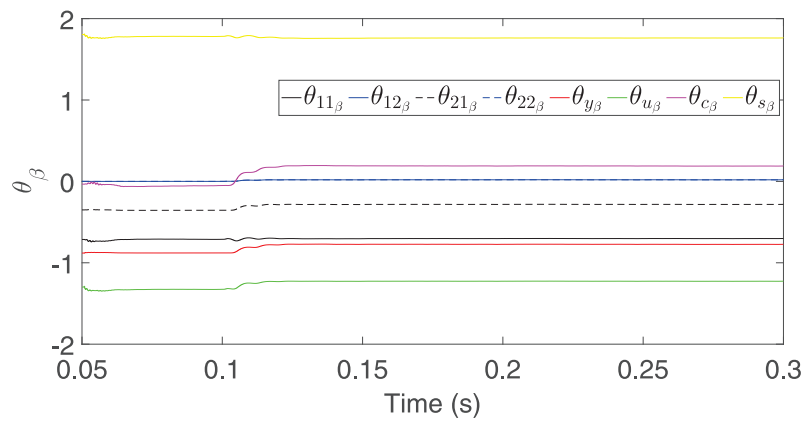
Figure 7 – Gains in β
Fonte: The author.

As expected, the gains presented more action on initial transient regime and at reference change instant, converging on steady state regime. The covariance matrices convergence are presented in Figures 8 and 9, for α and β coordinates, respectively.
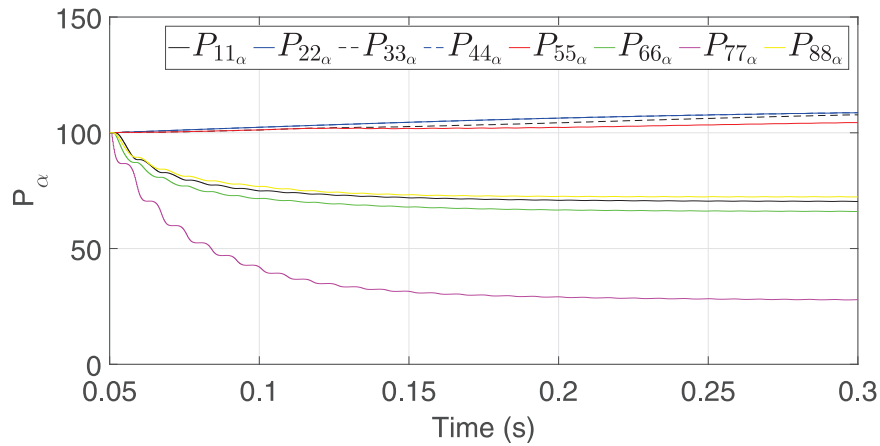
Figure 8 – Covariance matrix in α
Fonte: The author.
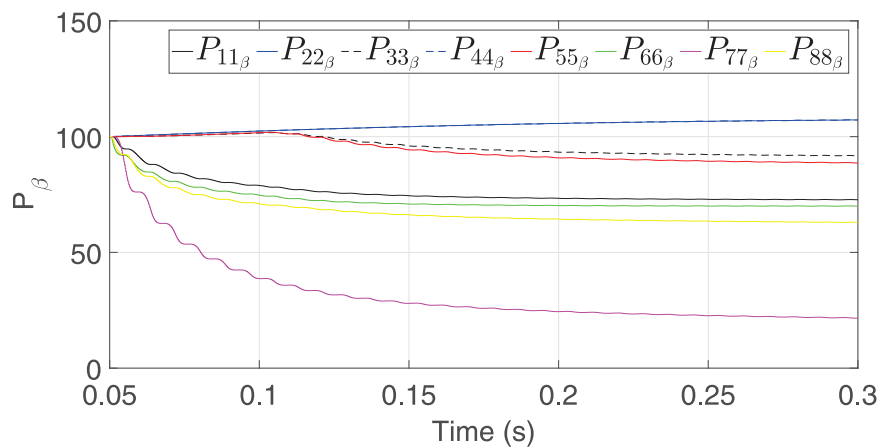
Figure 9 – Covariance matrix in β
Fonte: The author.

As can be noted, all parameters of gain vector and covariance matrix converged on steady state and remained with limited values on transient regimes, which means that majorant signal is robust enough to ensure boundedness of all closed-loop system signals. Finally, in Figure 10, the control actions are presented. Note that for grid disturbance rejection and properly reference tracking, no excessive efforts were required by the controller, even with unbalanced grid conditions, being feasible for experimental implementation.
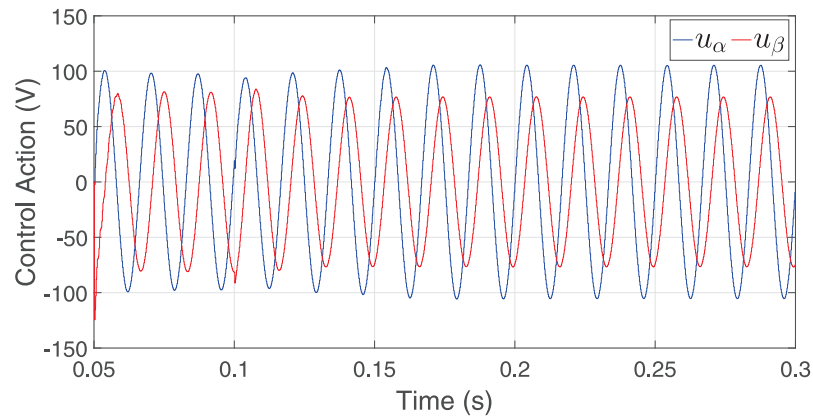
Figure 10 – Control actions in αβ
Fonte: The author.

5   Conclusion

In this work, it was presented a discrete-time direct Output Feedback-based LS-RMRAC for grid-injected currents control of a static 3-wire three-phase converter with LCL filter, under unbalanced grid voltage condition. The proposed method dealt properly with grid disturbances, parametric variations of grid impedance, even on unbalanced grid conditions. The proposed controller presented fast current tracking, with low initial overshoot and small tracking error on steady state, requiring feasible voltage to synthesize control action, considering many implementation aspects on simulation, such as: digital implementation delay, converter switching, grid uncertainties and grid voltage synchronization. Therefore, results indicate that it can be securely applied to experimental power plants. In a future work, controller design constraints will be investigated through Lyapunov' stability criterion.

REFERENCES

BELOV, A. Robust pole placement and random disturbance rejection for linear polytopic systems with application to grid-connected converters. **European Journal of Control**, Elsevier, v. 63, p. 116–125, 2022. Disponível em: <https://www.sciencedirect.com/science/article/abs/pii/S0947358021001199>.

BOSCH, S.; STAIGER, J.; STEINHART, H. Predictive current control for an active power filter with lcl-filter. **IEEE Transactions on Industrial Electronics**, IEEE, v. 65, n. 6, p. 4943–4952, 2017. Disponível em: <https://ieeexplore.ieee.org/abstract/document/8106670>.

CARDOSO, R. et al. Kalman filter based synchronisation methods. **IET generation, transmission & distribution**, IET, v. 2, n. 4, p. 542–555, 2008. Disponível em: <https://digital-library.theiet.org/content/journals/10.1049/iet-gtd_20070281>.

CRAMER, A. et al. Power grid simulation considering electric vehicles and renewable energy sources. In: IEEE. **2019 Fourteenth International Conference on Ecological Vehicles and Renewable Energies (EVER)**. 2019. p. 1–3. Disponível em: <https://ieeexplore.ieee.org/iel7/8798485/8813510/08813642.pdf>.

DANNEHL, J. et al. Investigation of active damping approaches for pi-based current control of grid-connected pulse width modulation converters with lcl filters. **IEEE Transactions on Industry Applications**, IEEE, v. 46, n. 4, p. 1509–1517, 2010. Disponível em: <https://ieeexplore.ieee.org/abstract/document/5471222>.

DANNEHL, J.; FUCHS, F. W.; THØGERSEN, P. B. Pi state space current control of grid-connected pwm converters with lcl filters. **IEEE Transactions on Power Electronics**, IEEE, v. 25, n. 9, p. 2320–2330, 2010. Disponível em: <https://ieeexplore.ieee.org/document/5443587>.

DUESTERHOEFT, W.; SCHULZ, M. W.; CLARKE, E. Determination of instantaneous currents and voltages by means of alpha, beta, and zero components. **Transactions of the American Institute of Electrical Engineers**, IEEE, v. 70, n. 2, p. 1248–1255, 1951. Disponível em: <https://ieeexplore.ieee.org/document/5060554>.

ELSAYAD, N.; MORADISIZKOOHI, H.; MOHAMMED, O. A. Design and implementation of a new transformerless bidirectional dc–dc converter with wide conversion ratios. **IEEE Transactions on Industrial Electronics**, IEEE, v. 66, n. 9, p. 7067–7077, 2018. Disponível em: <https://ieeexplore.ieee.org/document/8517159>.

EVALD, P. J. D. d. O.; TAMBARA, R. V.; GRÜNDLING, H. A. A discrete-time robust mrac applied on grid-side current control of a grid-connected three-phase converter with lcl filter. **ELECTRIMACS 2019: Selected Papers-Volume 1**, Springer Nature, v. 615, p. 45, 2020. Disponível em: <https://link.springer.com/chapter/10.1007/978-3-030-37161-6_4>.

EVALD, P. J. D. O.; TAMBARA, R. V.; GRÜNDLING, H. A. A direct discrete-time reduced order robust model reference adaptive control for grid-tied power converters with lcl filter. **Eletrônica de Potência**, Associação Brasileira de Eletrônica de Potência, v. 25, n. 3, p. 361–372, 2020. Disponível em: <https://sobraep.org.br/site/uploads/2020/09/rvol25no03-16-0039-361-372.pdf>.

FANG, X. et al. Improved quasi-y-source dc-dc converter for renewable energy. **CPSS Transactions on Power Electronics and Applications**, CPSS, v. 4, n. 2, p. 163–170, 2019. Disponível em: <https://ieeexplore.ieee.org/iel7/7873541/8758247/08758255.pdf>.

FLORA, L. D.; GRÜNDLING, H. A. Design of a robust model reference adaptive voltage controller for an electrodynamic shaker. **Eletrônica de Potência**, v. 13, n. 3, p. 133–140, 2008. Disponível em: <https://sobraep.org.br/site/uploads/2018/06/rvol13no3p1.pdf>.

GAO, C. et al. Current multi-loop control strategy for grid-connected inverter with lcl filter. In: IEEE. **33rd Youth Academic Annual Conference of Chinese Association of Automation (YAC)**. 2018. p. 712–716. Disponível em: <https://ieeexplore.ieee.org/document/8406464>.

GONZALEZ, J. M.; BUSADA, C. A.; SOLSONA, J. A. A robust controller for a grid-tied inverter connected through an lcl filter. **IEEE Journal of Emerging and Selected Topics in Industrial Electronics**, IEEE, v. 2, n. 1, p. 82–89, 2020. Disponível em: <https://ieeexplore.ieee.org/abstract/document/9160862>.

IOANNOU, P.; TSAKALIS, K. A robust direct adaptive controller. **IEEE Transactions on Automatic Control**, IEEE, v. 31, n. 11, p. 1033–1043, 1986. Disponível em: <https://ieeexplore.ieee.org/iel5/9/24237/01104168.pdf>.

IOANNOU, P. A.; SUN, J. **Robust adaptive control**. [S.l.]: Courier Corporation, 2012.

ISLAM, M.; GUO, Y.; ZHU, J. A high-frequency link multilevel cascaded medium-voltage converter for direct grid integration of renewable energy systems. **IEEE Transactions on Power Electronics**, IEEE, v. 29, n. 8, p. 4167–4182, 2013. Disponível em: <https://ieeexplore.ieee.org/document/6661455>.

ISLAM, M. R.; GUO, Y.; ZHU, J. A transformer-less compact and light wind turbine generating system for offshore wind farms. In: IEEE. **2012 IEEE international conference on power and energy (PECon)**. 2012. p. 605–610. Disponível em: <https://ieeexplore.ieee.org/abstract/document/6450285>.

JUNIOR, L. A. M. et al. Robust model predictive controller applied to three-phase grid-connected lcl filters. **Journal of Control, Automation and Electrical Systems**, Springer, v. 31, n. 2, p. 447–460, 2020. Disponível em: <https://link.springer.com/article/10.1007/s40313-019-00546-y>.

KHWAN-ON, S.; KONGKANJANA, K. The control of a multi-input boost converter for renewable energy system applications. In: IEEE. **2017 International Electrical Engineering Congress (iEECON)**. 2017. p. 1–4. Disponível em: <https://ieeexplore.ieee.org/document/8075782>.

LINDGREN, M.; SVENSSON, J. Control of a voltage-source converter connected to the grid through an lcl-filter-application to active filtering. In: IEEE. **29th Annual IEEE Power Electronics Specialists Conference (PESC)**. 1998. v. 1, p. 229–235. Disponível em: <https://ieeexplore.ieee.org/iel4/5671/15202/00701904>.

MACCARI, L. et al. Robust optimal current control for grid-connected three-phase pulse-width modulated converters. **IET Power Electronics**, IET, v. 8, n. 8, p. 1490–1499, 2015. Disponível em: <https://ietresearch.onlinelibrary.wiley.com/doi/10.1049/iet-pel.2014.0787>.

MACCARI, L. A. et al. Lmi-based control for grid-connected converters with lcl filters under uncertain parameters. **IEEE Transactions on Power Electronics**, IEEE, v. 29, n. 7, p. 3776–3785, 2013. Disponível em: <https://ieeexplore.ieee.org/abstract/document/6587559/>.

MOHAMMADI, S. et al. Optimal robust control of lcl-type grid-connected voltage source inverters against grid impedance fluctuations. In: IEEE. **10th International Power Electronics, Drive Systems and Technologies Conference (PEDSTC)**. 2019. p. 504–508. Disponível em: <https://ieeexplore.ieee.org/document/8697514>.

NAM, N. N. N. et al. Voltage sensorless model predictive control for a grid-connected inverter with lcl filter. **IEEE Transactions on Industrial Electronics**, IEEE, v. 69, n. 1, 2021. Disponível em: <https://ieeexplore.ieee.org/abstract/document/9324964>.

NEHRIR, M. et al. A review of hybrid renewable/alternative energy systems for electric power generation: Configurations, control, and applications. **IEEE Transactions on Sustainable Energy**, IEEE, v. 2, n. 4, p. 392–403, 2011. Disponível em: <https://ieeexplore.ieee.org/document/5773511>.

OSÓRIO, C. R. D. et al. Robust current control of grid-tied inverters affected by lcl filter soft-saturation. **IEEE Transactions on Industrial Electronics**, IEEE, v. 67, n. 8, p. 6550–6561, 2019. Disponível em: <https://ieeexplore.ieee.org/abstract/document/8825851>.

PINHEIRO, H. et al. Modulação space vector para inversores alimentados em tensão: uma abordagem unificada. **Sba: Controle & Automação Sociedade Brasileira de Automatica**, SciELO Brasil, v. 16, n. 1, p. 13–24, 2005. Disponível em: <http://www.scielo.br/scielo.php?script=sci_arttext&pid=S0103-17592005000100002>.

RAHBAR, K.; CHAI, C. C.; ZHANG, R. Energy cooperation optimization in microgrids with renewable energy integration. **IEEE Transactions on Smart Grid**, IEEE, v. 9, n. 2, p. 1482–1493, 2016. Disponível em: <https://ieeexplore.ieee.org/document/7544637>.

TAMBARA, R. V. et al. A discrete-time robust adaptive controller applied to grid-connected converters with lcl filter. **Journal of Control, Automation and Electrical Systems**, Springer, v. 28, n. 3, p. 371–379, 2017. Disponível em: <https://link.springer.com/article/10.1007/s40313-017-0313-3>.

TEODORESCU, R.; LISERRE, M.; RODRÍGUEZ, P. **Grid Converters for Photovoltaic and Wind Power Systems**. Wiley & Sons – IEEE, 2011. Disponível em: <https://www.wiley.com/en-us/Grid+Converters+for+Photovoltaic+and+Wind+Power+Systems-p-9780470057513>.

TIWARI, S. K.; SINGH, B.; GOEL, P. K. Design and control of microgrid fed by renewable energy generating sources. **IEEE Transactions on Industry Applications**, IEEE, v. 54, n. 3, p. 2041–2050, 2018. Disponível em: <https://ieeexplore.ieee.org/document/8258886>.

TRAN, T. V.; YOON, S.-J.; KIM, K.-H. An lqr-based controller design for an lcl-filtered grid-connected inverter in discrete-time state-space under distorted grid environment. **Energies**, Multidisciplinary Digital Publishing Institute, v. 11, n. 8, p. 2062, 2018. Disponível em: <https://www.mdpi.com/1996-1073/11/8/2062>.

DADOS DO AUTOR

Nome: Paulo Jefferson Dias de Oliveira
E-mail: paulo.evald@gmail.com
Lattes: http://lattes.cnpq.br/1946704909213416
Pesquisador no Pós-Doutorado no Programa de Pós-Graduação em Computação da Universidade Federal do Rio Grande (FURG), Doutor em Engenharia Elétrica pela Universidade Federal de Santa Maria (UFSM), Mestre em Engenharia de Computação e Engenheiro de Automação pela FURG. Suas áreas de interesse são Teoria de Controle, Controle Aplicado, Modelagem de Sistemas Dinâmicos e Sistemas de Energias Renováveis.